Q. J. R. Meteorol. Soc. (1999), **125**, pp. 967–991

Severe flooding over central and southern Greece associated with pre-cold frontal orographic lifting

By V. KOTRONI[1]*, K. LAGOUVARDOS[1], G. KALLOS[1] and D. ZIAKOPOULOS[2]
[1]*University of Athens, Greece*
[2]*Hellenic National Meteorological Service, Greece*

(Received 16 February 1998; revised 13 July 1998)

SUMMARY

An extreme rainfall event, associated with a cold front, which occurred on 11–12 January 1997 over Greece is investigated through observational analysis and numerical simulations. The analysed storm system produced large amounts of rainfall, with devastating impacts over central and southern Greece, where at some sites 24-hour accumulated precipitation exceeded 300 mm. The model analysis was performed with the three-dimensional non-hydrostatic Colorado State University Regional Atmospheric Modeling System. The model results caught the larger-scale features present in the observational analyses while developing more realistic finer-scale features. Sensitivity tests are also performed in order to investigate the role of the topography of the Greek peninsula on the enhancement of convection. Indeed, the orientation of the flow was optimal for advection of moist air with a maximized fetch over the sea, and at an angle of impact optimum for orographic lifting ahead of the main topographic axes of continental Greece.

KEYWORDS: Convection Numerical modelling Precipitation

1. INTRODUCTION

Heavy precipitation events have become the second most significant natural disaster problem in Greece after the frequent and sometimes destructive earthquakes. During the last five years at least one major precipitation event per year occurred over Greece. Some of these events have been already reported in the literature (e.g. Lagouvardos *et al.* 1996; Petroliagis *et al.* 1996; Prezerakos *et al.* 1997). Systems accompanied by torrential rains over the Mediterranean have been the object of study in the past. Senesi *et al.* (1996) presented a detailed mesoscale analysis of the Vaison-La-Romaine flash flood in 1992 over southern France, based on radar data analysis and extensive modelling. Barret *et al.* (1994) provided a description of a flash flood which occurred almost over the same region one year later. The authors concluded that this event was generated by a combination of several mesoscale convective systems ahead of a slow-moving cold front associated with a cut-off low. Lagouvardos *et al.* (1996) presented successful simulations of a major flooding event over Greece in October 1994 using two numerical models, while Petroliagis *et al.* (1996) discussed the European Centre for Medium-Range Weather Forecasts (ECMWF) Ensemble Prediction System (EPS) forecast capability for the same flash flood over Greece. All the aforementioned papers underlined the fact that unstable synoptic conditions were reinforced by warm and moist advection due to southerly winds driving moist air masses from the warm Mediterranean sea toward the northern Mediterranean coasts.

On 11 and 12 January 1997 a major precipitation event occurred over the eastern Mediterranean and especially over southern Greece. Heavy precipitation (more than 300 mm of accumulated rain within the 24 hours, ending at 1800 UTC 12 January 1997, Fig. 1(c)) provoked severe damage over southern Greece in Peloponnisos, where several cities (such as Korinthos, among others) experienced severe flooding. Flooding was not only restricted to Peloponnisos. Heavy precipitation (e.g. 200 mm within 24 hours in Desfina, and 100 mm near Lamia) caused severe problems to the road network of central Greece where some bridges collapsed, while in Athens flooding was reported in some suburban areas (more than 70 mm of rainfall within a few hours).

* Corresponding author: University of Athens, Laboratory of Meteorology, Panepistimioupolis, Bldg. PHYS-V, 15784 Athens, Greece.

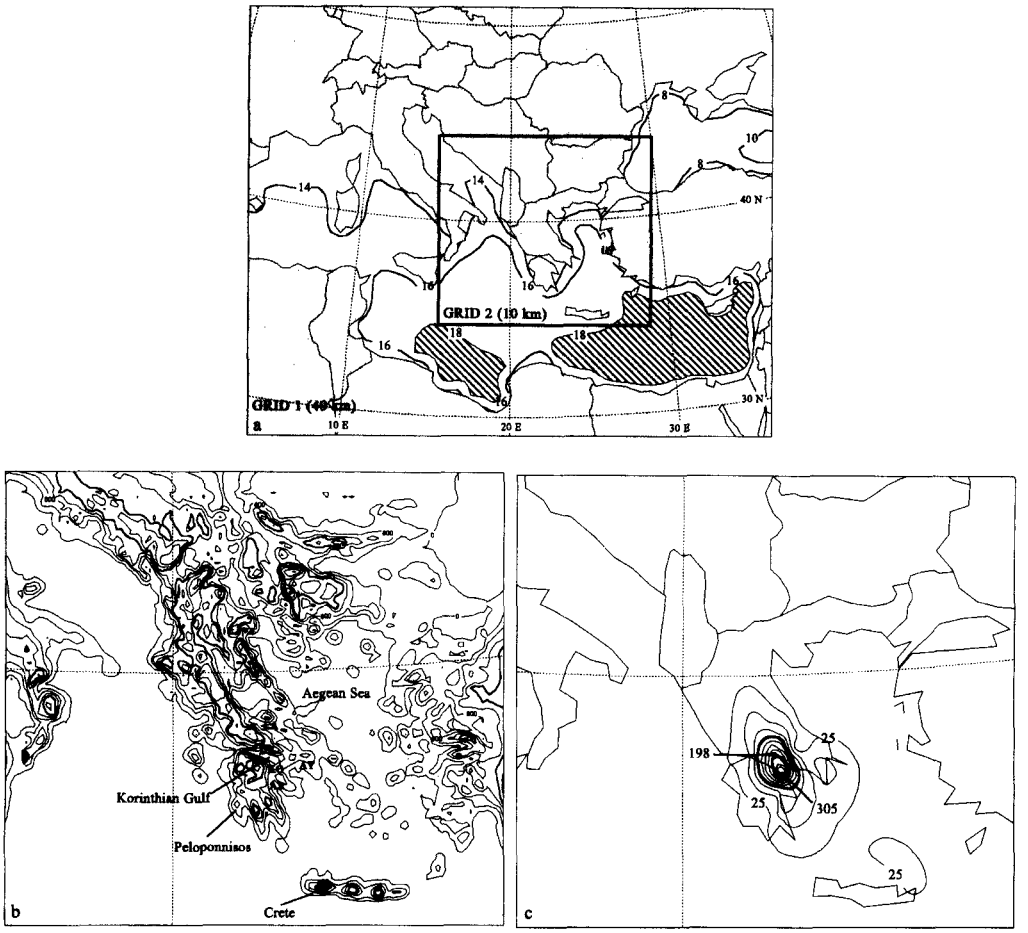

Figure 1. (a) Horizontal extent of the Regional Atmospheric Modeling System (RAMS) two nested grids (Grid 1, Grid 2). For each grid the horizontal grid increment is also given. The sea surface temperature field used by the model is also reported at 2 degC intervals. Values greater than 18 °C are hatched. (b) Topography inside the second grid of the RAMS (at 300 m intervals). The bold line denotes the 1200 m isoline. LA, DE, KO, AR and AT, refer to Lamia, Desfina, Korinthos, Argos and Athens stations (see text for further details). (c) 24-hour accumulated precipitation ending at 1800 UTC 12 January 1997 (at 25 mm intervals) from a network of 59 rain-gauges. The 100 and 200 m isolines are in bold. The accumulated precipitation at the Korinthos and Desfina stations (305 mm and 198 mm respectively) is shown.

The 11–12 January precipitation event was associated with the passage of a low-pressure system south of Greece, accompanied by a slow-moving cold front. The ECMWF operational system predicted accurately the depth and positioning of the surface low three days in advance, providing also indication for a major rainfall event, although local extreme values were not represented (Lanzinger 1997). This operational product was also assisted by the ECMWF EPS where more than half of the ensemble members predicted high amounts of accumulated precipitation over eastern continental Greece.

This work was limited not only by the severity but also mainly by the interesting spatio–temporal variability of the precipitation event. Indeed:

• About one half of the total precipitation accumulated well before the arrival of the cold front over Greece. Then, precipitation associated with the frontal passage, falling over an already saturated soil, led to serious flooding.

• The heaviest precipitation occurred over the coastal areas on the north and south coasts of the Korinthian Gulf, upstream of important mountain barriers.

Thus the aim of this study is to investigate the physical mechanisms responsible for the aforementioned features of the 11–12 January 1997 event.

Since events with extreme intensity occur only a few times over the year, researchers and operational forecasters must rely on the detailed analysis of case-studies in order to gain a deep understanding of the dynamics controlling the behaviour of these systems. With this aim the 11–12 January 1997 flooding event is studied in this paper through both observational and model analysis. The synoptic description of the event is based on all available observations (surface, upper-air and satellite data) as well as on ECMWF $0.5^\circ \times 0.5^\circ$ upper-air analyses. The mesoscale analysis of the event is based on nested-grid simulations performed with the Regional Atmospheric Modeling System (RAMS). The role of topography of the Greek peninsula on the enhancement of convection, especially near the coasts upwind of the mountains, is investigated through sensitivity tests using the RAMS. Indeed the enhanced precipitation over the sea, or the coast upwind of mountains, seems to be strongly related to orography, as reported by Ogura *et al.* (1985) and Watanabe and Ogura (1987) over Japan, Grossman and Durran (1984) over India, and Caracena *et al.* (1979) over the USA. The authors have attributed the analysed severe thunderstorms and deep convection midway between the mountain peaks and the shore or even offshore, to the forced lifting of moist air directly to its lifting condensation level (LCL) when this is near or below the top of the mountain barrier.

The present work is organised as follows: section 2 is devoted to the synoptic description of the event, based on available observations and inspection of the ECMWF gridded analyses. The analysis of the frontal mesoscale structure, based on model results, is presented in section 3. In the same section a brief description of the RAMS and the specific settings for the present application are presented. The results of sensitivity tests are also discussed in this section. Finally, concluding remarks as well as a conceptual model describing the airflow associated with this event are presented in the last section.

2. Synoptic description

This section provides an observational description of the evolution of the frontal system and the development of the flood event (based on all available observations as well as on ECMWF upper-air analyses) with the aim of presenting the general features of the phenomenon as well as providing a basis for verifying the RAMS results presented in section 3. The low centre which affected Greece was emanating from a low centre which on 9 January 1997 was centred over the Gulf of Lion in the north-western Mediterranean (not shown). During the following days this low centre progressed south-eastward along the west coast of Italy and on 11 January was located over Sicily. This is a primary track for cyclones originating from the Gulf of Lion which then affect the Ionian Sea (Brody and Nestor 1980).

The mean-sea-level pressure analysis from the ECMWF, at 0000 UTC 12 January 1997, shows a low-pressure centre of 1009 hPa located over Sicily, with an associated cold front extending from the low-pressure centre down to the north African coasts (Fig. 2(a)). At the surface an intense south-easterly wind prevails ahead of the cold front, covering almost the entire part of the eastern Mediterranean (not shown). Moreover a high-pressure

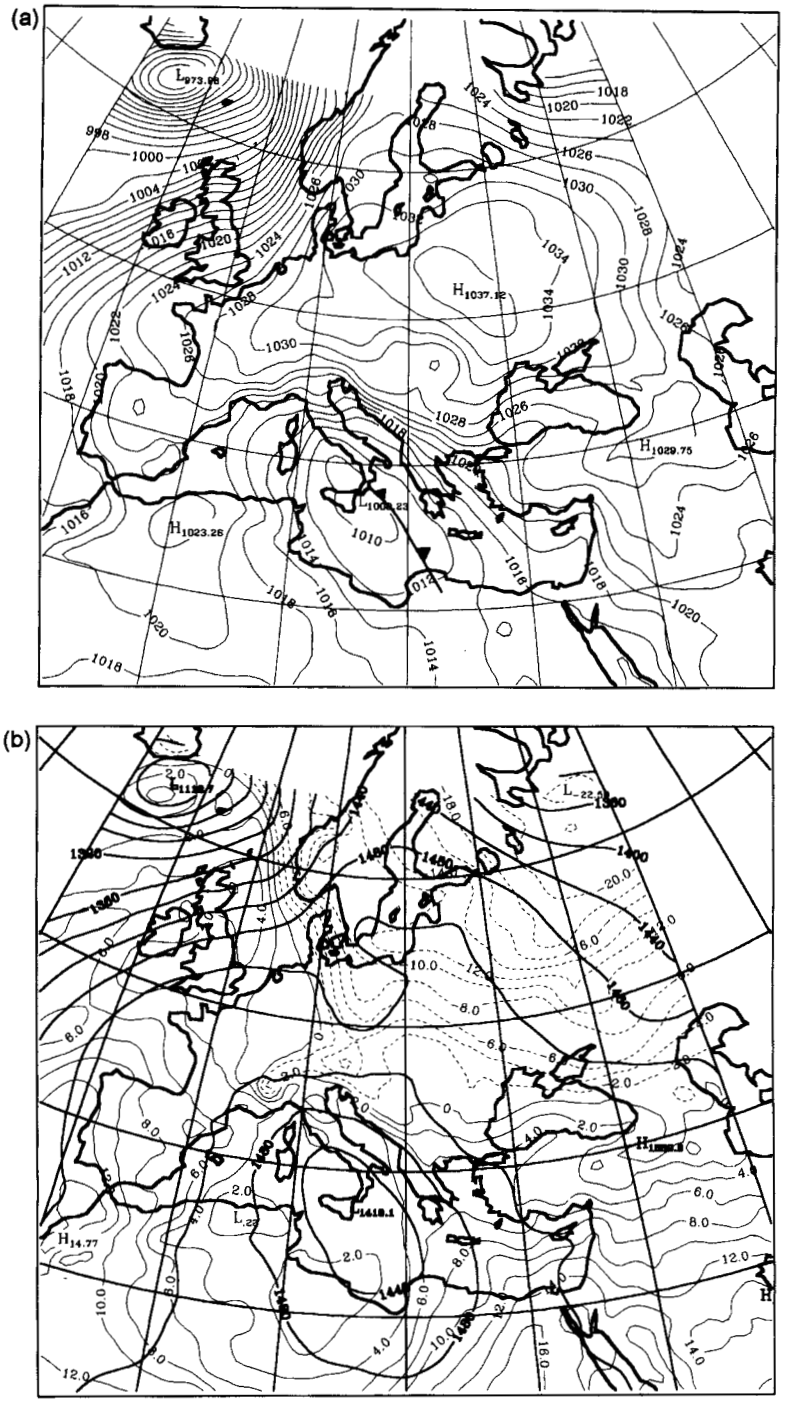

Figure 2. The ECMWF analyses valid at 0000 UTC 12 January 1997 of (a) mean-sea-level pressure (hPa); (b) 850 hPa geopotential height (bold lines, m) and temperature (solid line, °C, negative values are dashed); and (c) 500 hPa geopotential height (m) and isotachs at 300 hPa (light shading: >45 m s^{-1}, medium shading: >50 m s^{-1}, dark shading: >55 m s^{-1}).

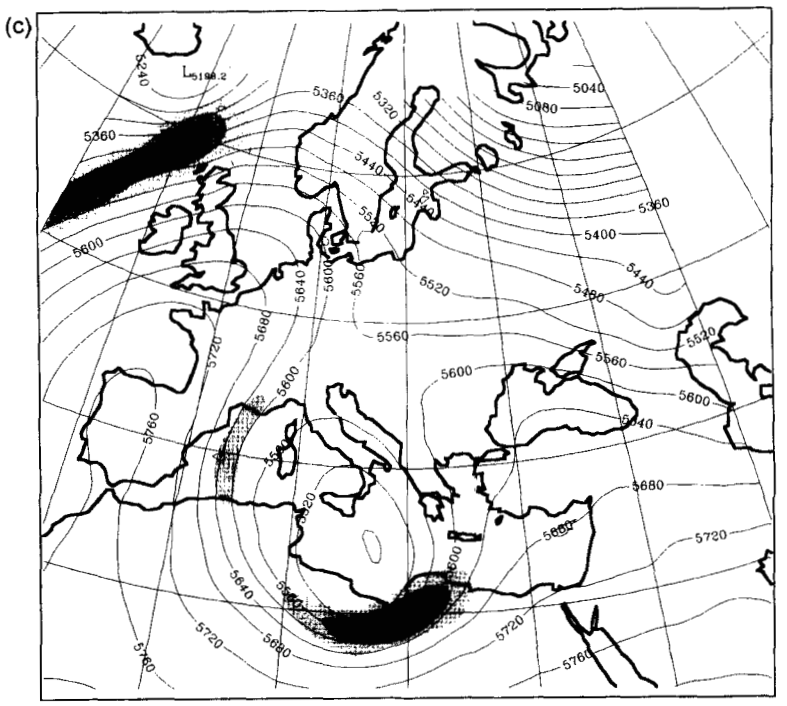

Figure 2. Continued.

system (1037 hPa) over north-eastern Europe is extending southwards over the Balkans. The associated cold-air advection and north-easterly surface flow over the eastern Balkans and northern Greece prohibit the north-eastward propagation of the low-pressure system. Indeed the climatological study of Ionian Sea cyclones performed by Brody and Nestor (1980) revealed that these cyclones are directed eastwards across the southern Aegean Sea (instead of a more likely path north-eastwards across Greece) when there is a cold surge to the north as was the case during this specific event. This type of path was also presented in the climatological analysis of cyclone tracks for the period 1982–87 as performed by Alpert *et al.* (1990). At the 850 hPa level (Fig. 2(b)) a moderate temperature gradient is evident in the area just over the position of the front at the surface, with prominent warm-air advection over the eastern Mediterranean (east of the 20°E meridian). At the 500 hPa level a cut-off low of 5480 gpm height is located north of the Gulf of Sidra, while a ridge is observed over the western coasts of Europe (Fig. 2(c)). A rather intense jet streak is evident at the 300 hPa level around the cut-off low, with a maximum of 54 m s^{-1} observed over the northern Libyan coasts. This upper-level feature is located far to the southern edge of the surface cold front and no interaction is expected with the low-level flow associated with the front itself and the frontal convection; this is also supported by satellite imagery (discussed in the next paragraph).

An enhanced Meteosat infrared picture at the same time (0000 UTC 12 January) is presented in Fig. 3(a). The most interesting feature on this figure is the appearance of two distinct bands of high convective clouds, one over the maritime area west of Greece, associated with the cold front depicted on the surface chart (Fig. 2(a)), the other an important cloud cluster over the eastern part of continental Greece and southern Aegean Sea. The

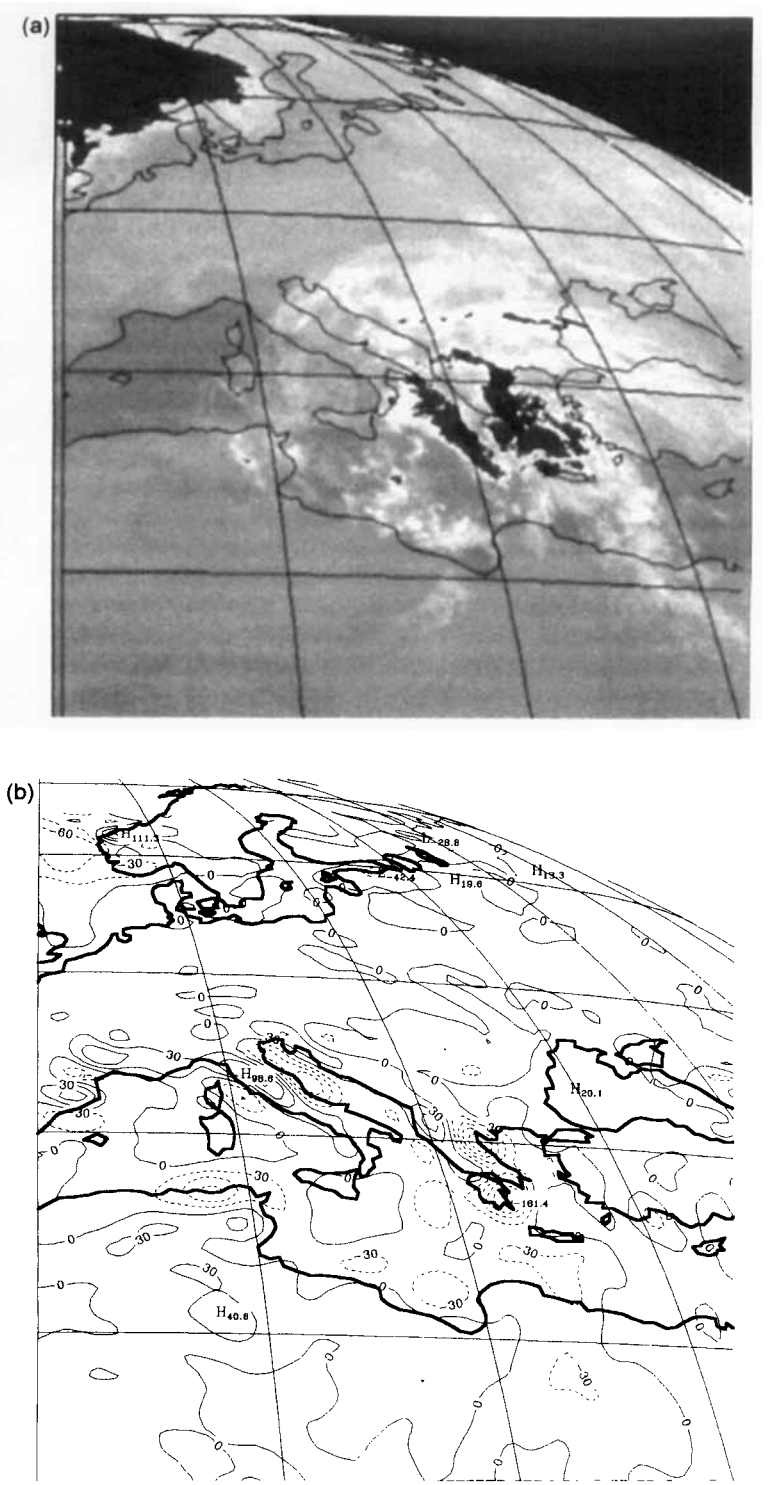

Figure 3. (a) Meteosat enhanced infrared satellite image and (b) the ECMWF analysis of vertical velocity at the 850 hPa level (Pa s^{-1}). Dashed lines denote negative values (ascending motions). Both valid at 0000 UTC 12 January 1997.

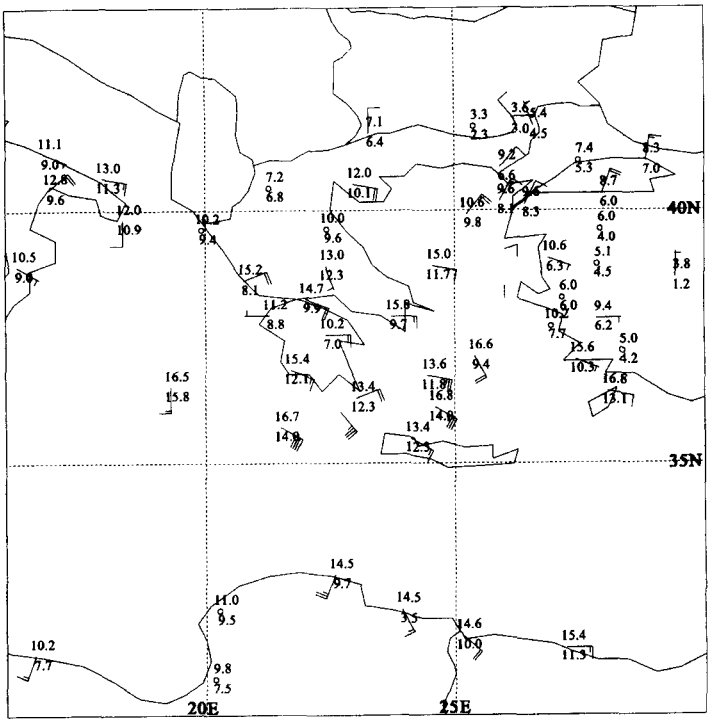

Figure 4. Surface synoptic reports of temperature (upper figures) and dew-point temperature (lower figures) (°C), and wind (one pennant: 20 m s^{-1}, one barb: 4 m s^{-1}, one half-barb: 2 m s^{-1}), valid at 0000 UTC 12 January 1997.

highest cloud tops (dark shading in Fig. 3(a)) are observed over central Greece, northern Peloponnisos and the Korinthian Gulf. An almost convective cloud-free area is depicted between the two bands of clouds, over western Greece and Albania, with a characteristic width of approximately 150 km. The 850 hPa vertical velocity provided by the ECMWF, plotted on the same projection as the satellite imagery, is shown in Fig. 3(b). As can be seen, there is very good agreement between the ascending motions in the lower troposphere and the cloud structure. Strong ascending motions are evident over eastern Greece, and moderate ascent ahead of the surface cold front, while moderate subsiding motions are evident over western Greece. These subsiding motions (a downslope flow along the lee of the mountain range) result from the interaction of the easterly/south-easterly flow with the mountain barriers of the Greek peninsula (Fig. 1(b)). These subsiding motions are likely to explain the suppression of deep convection over western Greece.

Figure 4 depicts surface and ship observations valid at 0000 UTC 12 January 1997. Ships located just ahead of the cold front reported warm (>16 °C) and moist air masses (with a dew-point depression of 0.7 degC). Another important feature is the strong south-eastern flow east of the 20°E meridian, and in the warm sector of the front, which exceeded 16 m s^{-1}, conveying warm and moist air masses towards the south-eastern part of the Greek peninsula. As discussed in detail later, the interaction of this airflow with the steep topography produced large amounts of rain over the area. At that time heavy precipitation had started to be recorded at numerous synoptic stations, mainly over Peloponnisos. Two cities in north-eastern Peloponnisos (Argos and Korinthos, see Fig. 1(b)) reported heavy rain beginning at 0000–0100 UTC 12 January, as well as flooding. Moderate rain

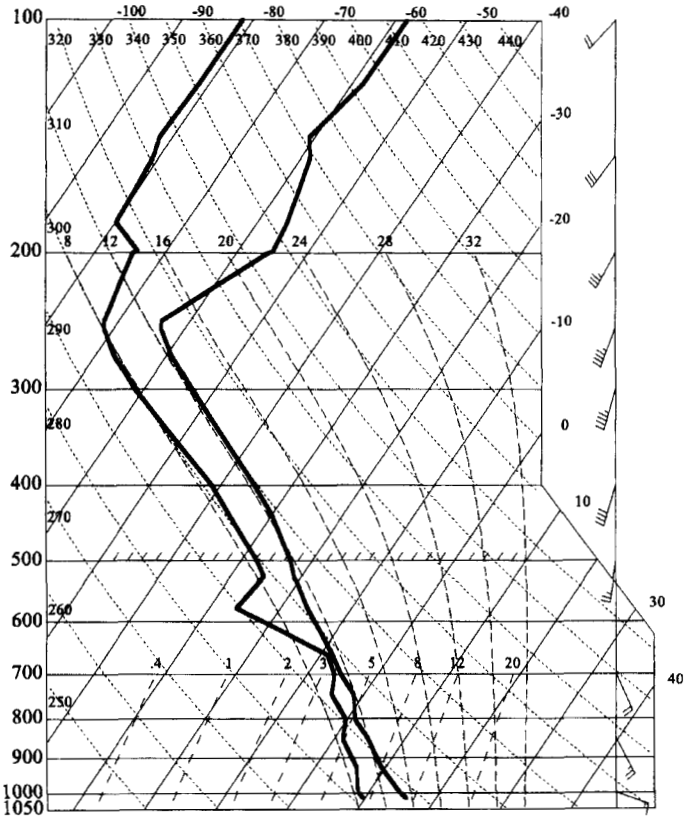

Figure 5. Skew-T log P diagram constructed from the 0000 UTC 12 January 1997 sounding released from Athens (one barb: 4 m s^{-1}, one half-barb: 2 m s^{-1}).

was reported in northern Crete while thunderstorm activity was reported over central and northern Greece, but without significant amounts of precipitation at the ground. At that time, significant weather and rain were not reported over the western part of the country (over the cloud-free area depicted in Fig. 3(a)) or over the Aegean Sea.

The 0000 UTC 12 January 1997 sounding released at Athens was located well ahead of the surface cold front, but it is representative of the moist flow being advected over the Aegean Sea (Fig. 5). The low levels are relatively moist, showing weak static stability, the LCL is at 928 hPa and the level of free convection (LFC) at 850 hPa, showing that the atmosphere was ready to release its potential instability with only a little lifting. The troposphere is moist up to 650 hPa and almost saturated in the layer 700–650 hPa. From 500 hPa upwards the atmosphere shows a weak stability to moist ascent. All calculated stability indices (Showalter, K-index, Jefferson, Boyden, Pickup, Totals index) indicate the potential for severe convective activity over the region. Winds were veering with height, with a characteristic south-easterly flow from the ground up to the 700 hPa level, with further veering to a south-westerly flow above this level.

Twelve hours later, at 1200 UTC 12 January 1997, the low centre of 1008 hPa had moved to a position south-west of Greece, approximately at 35°N, 20°E, while the associated cold front had slowly progressed over the area south of Peloponnisos, over Crete and towards the north African coasts (Fig. 6(a)). The pressure gradient had intensified

over the central and southern Aegean Sea. Warm advection is evident at the 850 hPa level (Fig. 6(b)) over the Aegean Sea, and the moist airflow is directed at a significant angle towards the mountain barriers of central Greece and Peloponnisos. Note also a packing of the isotherms and cold-air intrusion over the Balkans and northern Greece associated with the north-easterly flow prevailing over the area. The cut-off low of 5470 gpm had also progressed eastwards, close to the 20°E meridian and covering the central Mediterranean, without further deepening, while the upper-level jet streak (evident at the 300 hPa level) had maintained its east–west orientation over north Africa, while its intensity had increased to 60 m s^{-1} (Fig. 6(c)).

The enhanced Meteosat infrared picture at 1200 UTC 12 January (Fig. 7(a)) shows a uniform and extended cloud mass over eastern and southern Greece, and over the southern Aegean Sea. The cloud tops are covering a much wider area than 12 hours before, having a north-west/south-east orientation from southern continental Greece over the western Aegean Sea and eastern Crete. The edge of the convective clouds over the sea follows very well the cold front analysed at that time on the surface chart (see Fig. 6(a)). The ECMWF vertical-velocity field at the 850 hPa level shows again the strong ascending motions over the eastern part of continental Greece down to the southern Aegean Sea, with a strong maximum over the Attica peninsula (Fig. 7(b)). Descent is evident over the whole western part of the Greek peninsula.

The surface-network reports at 1200 UTC 12 January (Fig. 8) show an intensified south-easterly flow over the south Aegean Sea (wind intensity >16 m s^{-1}, north of Crete), further feeding the system with moisture loaded after a long fetch over the Mediterranean waters. Over north-eastern Greece and the northern Aegean Sea there is also a strong north-easterly flow advecting cold air, and converging over the central Aegean with the south-easterly flow. At that time, heavy rain and thunderstorms were reported from almost all stations located east of the main topographic axis of the Greek peninsula (see Fig. 1(b) for the topographic characteristics of the area), with the most violent phenomena over Athens, eastern Peloponnisos and over the Korinthian Gulf. As shown in Fig. 1(c), the greater amounts of precipitation were accumulated over northern Peloponnisos and central Greece. High precipitation amounts were also accumulated over the Athens Basin, and significant flooding was reported in some suburban areas of Athens. However, the major disasters were reported after 1200 UTC 12 January in the city of Korinthos in northern Peloponnisos, with severe flooding in the major part of the city and also near Lamia city in central Greece where the flash flood provoked the collapse of several road bridges in the Sperhios river basin west of the city.

A better overview of the evolution of rainfall over northern Peloponnisos can be achieved through inspection of the hourly accumulated precipitation reported by a synoptic station near Korinthos (Fig. 9). A peak of 33 mm was registered at 0000 UTC 12 January, with heavy precipitation lasting up to 0500 UTC 12 January, while a secondary maximum of 31.5 mm was registered at 1100 UTC 12 January. This second maximum occurred over an already saturated soil and provoked the severe flooding in the city of Korinthos during the afternoon hours of 12 January.

Finally, Fig. 10 presents the skew$T$–log$P$ diagram constructed from the 1200 UTC 12 January Athens sounding. The entire troposphere is very moist, the LCL is at 941 hPa and the LFC at 920 hPa, 70 hPa lower than its position 12 hours before, indicating that a minor upward displacement of the air could lead to free convective motions. Below the LCL the layer shows an almost neutral stability. From the calculation of various indices (Showalter, K-index, Jefferson, Boyden, Pickup, Totals index) there is an indication for potential severe convection over the region. The convective available potential energy was estimated to be 880 J kg^{-1}. Moreover, the south-easterly flow, conveying moist air through

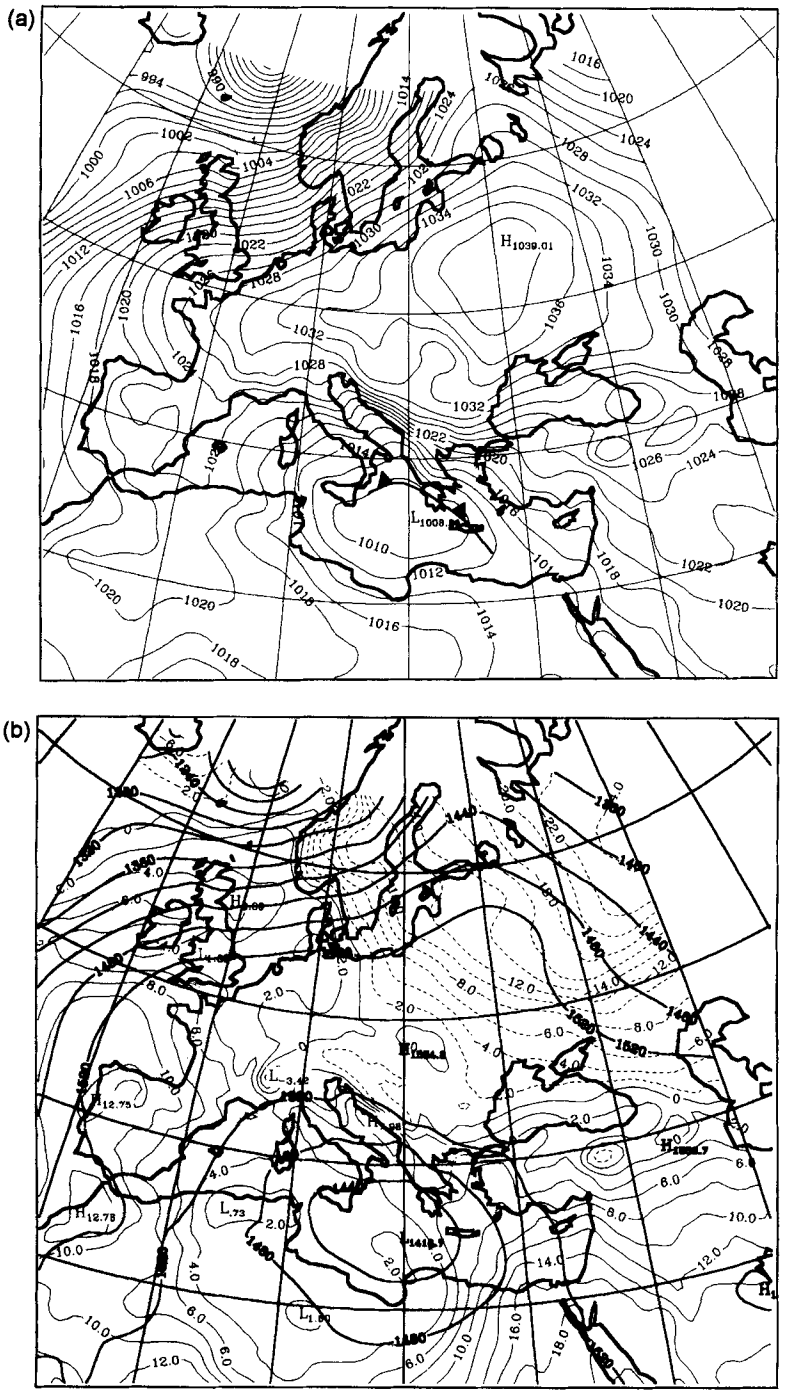

Figure 6. As Fig. 2 but for 1200 UTC 12 January 1997.

(c)
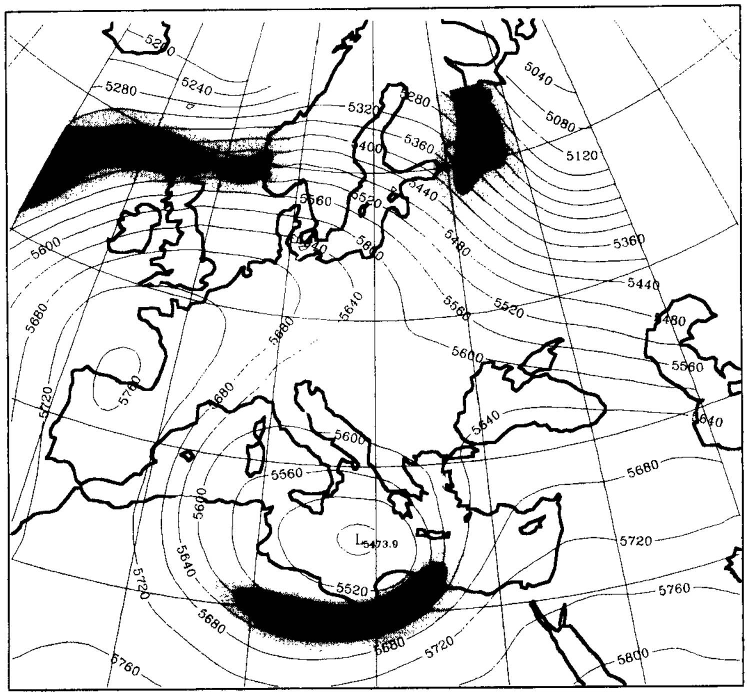

Figure 6. Continued.

its path over the Mediterranean, is now stronger than 12 hours before and extends from the ground up to the 500 hPa level.

3. Mesoscale analysis

(*a*) *Description and set-up of the RAMS*

The RAMS was developed at the Colorado State University and at the ASTER Division of Mission Research Corporation as a research model, but recently it is starting to be used also as an operational model (e.g. Cotton *et al.* 1994; Tremback *et al.* 1994). A detailed description of the model physics and application fields is given by Pielke *et al.* (1992).

For the present application, the RAMS was initialized at 1200 UTC 11 January 1997 and the duration of the simulation was 36 hours. The nonhydrostatic version of the model was used and two nested grids were defined. Indeed the computational domain of the model consisted of:

(i) the outer grid, with a mesh of 76 × 62 points and a 40 km horizontal grid interval, centred at 40°N latitude and 20°E longitude, and

(ii) the inner grid, with 122 × 110 points and a 10 km horizontal grid interval, centred at 39°24″N latitude and 22°24″E longitude.

The extent of both grids with the detailed topography of the inner grid is shown in Figs. 1(a) and 1(b) respectively. Twenty-five levels that followed the topography were used on all grids. The vertical spacing varied from 120 m near the surface to 1 km at the top of

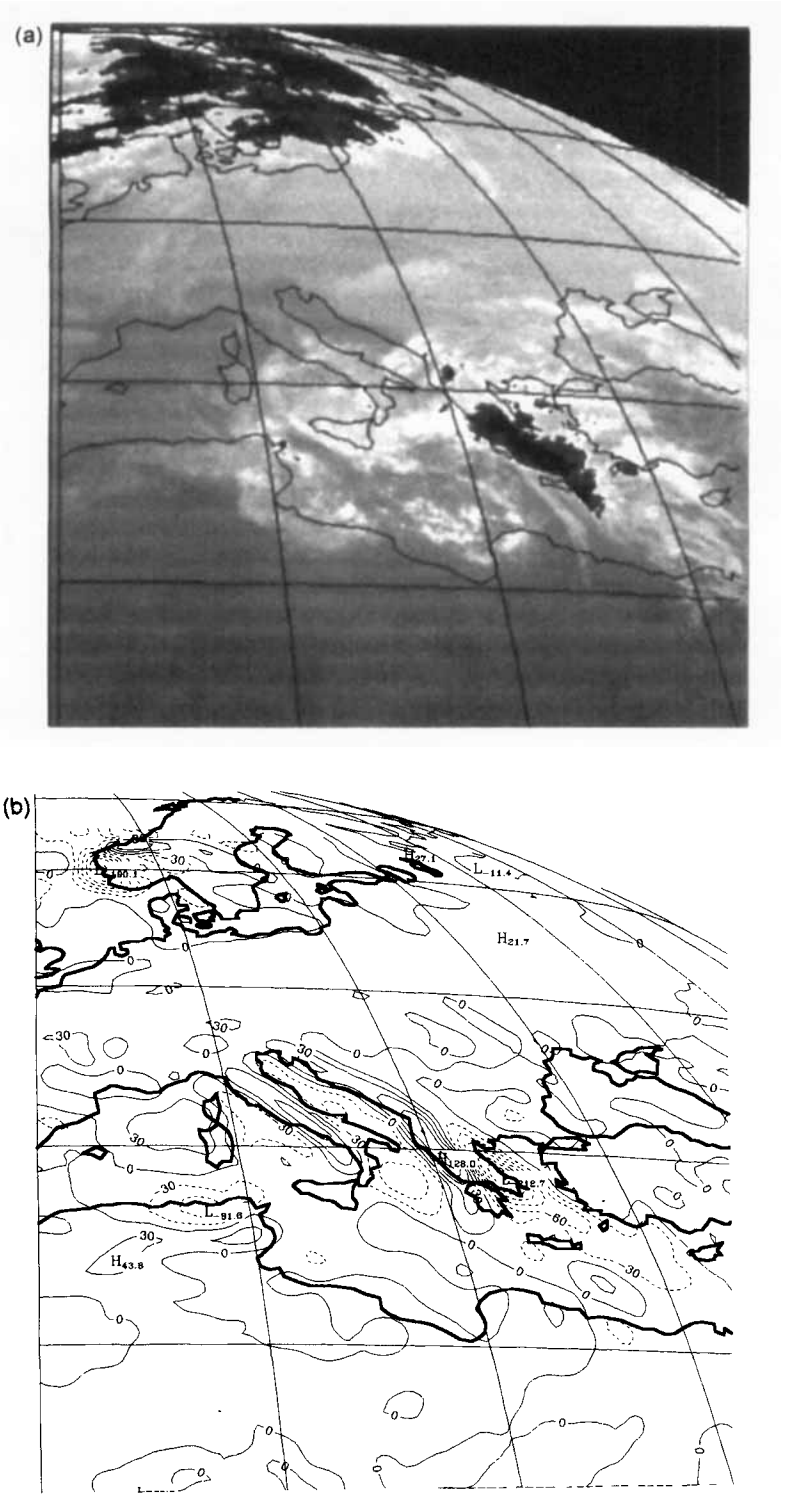

Figure 7. As Fig. 3 but for 1200 UTC 12 January 1997.

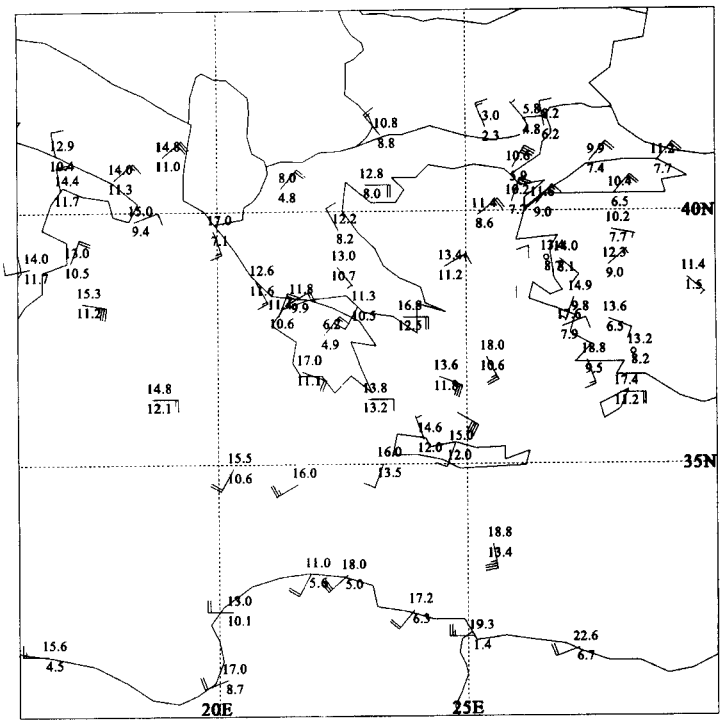

Figure 8. As Fig. 4 but for 1200 UTC 12 January 1997.

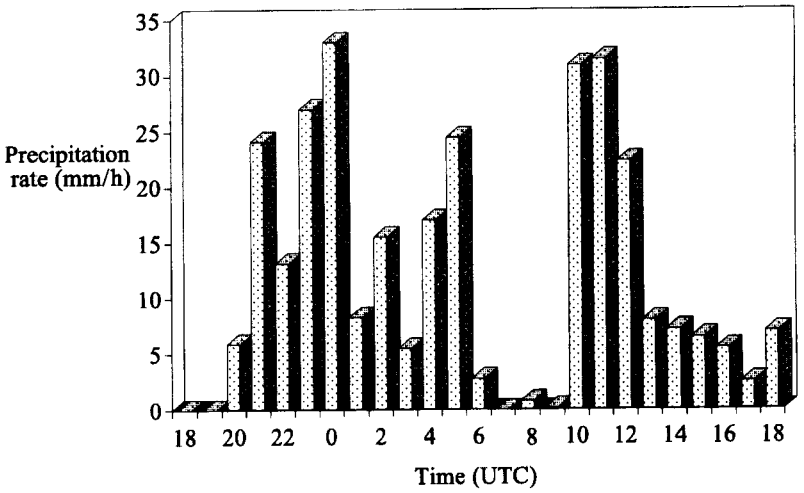

Figure 9. Temporal evolution of precipitation rate recorded by the Korinthos surface station from 1800 UTC 11 January to 1800 UTC 12 January 1997.

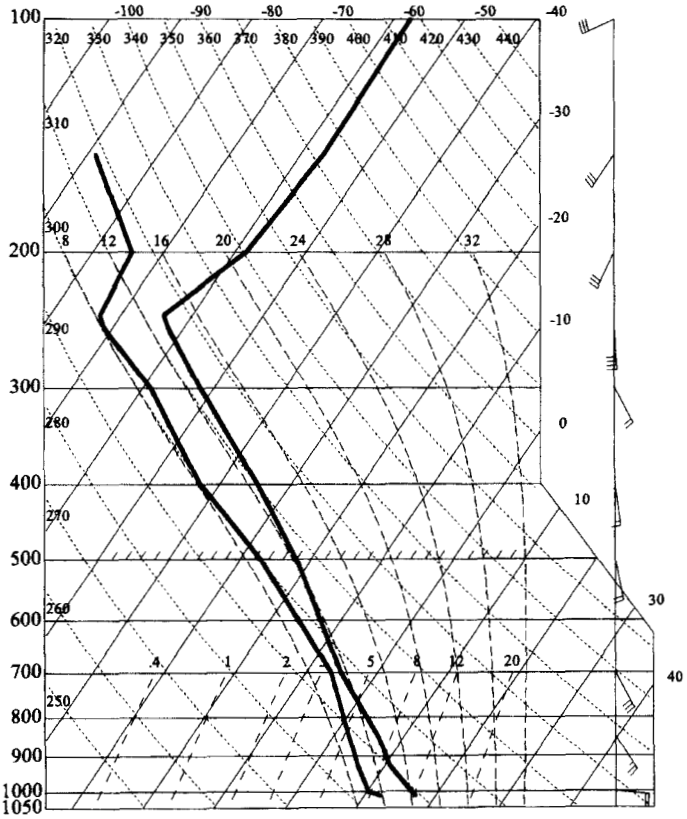

Figure 10. As Fig. 5 but for the 1200 UTC 12 January 1997 sounding.

the model domain ($z = 15.5$ km). Along with these settings, other RAMS configuration options include:

- The relaxation scheme similar to Davies (1976) was used for the lateral boundary conditions on the outer grid.
- A rigid lid was set at the model top boundary while top-boundary nudging (which damps gravity waves) was activated.
- A soil layer was used to predict the sensible- and latent-heat fluxes at the soil–atmosphere interface (McCumber and Pielke 1981; Avissar and Mahrer 1988). Six soil levels were used down to 50 cm below the surface.
- The full microphysical package of the RAMS was activated (Walko *et al.* 1995). This package includes the condensation of water vapour to cloud water when supersaturation occurs as well as the prognosis of rain, graupel, pristine ice, aggregates, and snow species.
- A modified Kuo-type cumulus parametrization developed by Tremback (1990) was used because the model-resolved convergence produced at the scales of the outer (40 km) grid is not enough to initiate convection explicitly.

The ECMWF $0.5° \times 0.5°$ gridded analysis fields are objectively analysed by the RAMS model on isentropic surfaces from which they are interpolated to the RAMS grids; they were then used to initialize the model. The 6-hourly ECMWF analyses were linearly interpolated in time in order to nudge the lateral boundary region of the RAMS coarser grid at a nudging time-scale of one hour. Observed sea surface temperature data of $1° \times 1°$

resolution provided by the ECMWF were used (see Fig. 1(a) for the horizontal distribution of sea surface temperature). Moreover, topography derived from a $30'' \times 30''$ terrain data and gridded vegetation type data of $10' \times 10'$ resolution was used.

The aforementioned set-up constitutes the control run (CONTROL hereafter). In order to test the role of topography on the enhancement of precipitation, a sensitivity test was carried out. This test (called NOTOPO hereafter) was identical to CONTROL but with one exception; the domain topography was set to zero, but the land–sea distribution was exactly the same as in CONTROL. In order to eliminate the effect of terrain on the initial conditions, the RAMS pre-processor was rerun in order to regenerate the initial and boundary conditions based on zero terrain heights for NOTOPO. Results from both experiments are discussed in the following sub-sections.

(*b*) *RAMS results—CONTROL run*

The inflow of warm and moist air in the lower tropospheric levels from the south-eastern Mediterranean towards Greece is evident in the 925 hPa wind and equivalent potential temperature (θ_e) field of the outer grid of the RAMS at 0000 UTC 12 January (Fig. 11). The main characteristics of the two fields are:

- A strong south-easterly moist flow that covers the eastern Mediterranean and extends northwards to the Aegean Sea and to the eastern coasts of central Greece (Figs. 11(a) and (b)). Note that the 308 K θ_e isoline characterizes the area over the warmest eastern Mediterranean waters (>18 °C, see hatched areas in Fig. 1(a)), indicating that the moisture load of the lower tropospheric air masses is directly related to the moisture supply from the sea. Indeed, inspection of the mixing-ratio distribution during the whole simulation period revealed that the moister air masses which initially were confined over the warmest eastern Mediterranean waters had been gradually advected north-westwards to the Greek peninsula by the strong south-easterly low-level flow. This belt of warm and moist air masses makes up the 'warm conveyor belt' of the cold front as termed by Browning and Pardoe (1973). The south-easterly flow, in the lower layers, after its long fetch over the Mediterranean waters, is subject to coastal convergence due to increased surface friction over land, which is believed to enhance rainfall. However, forced upslope lifting by the Greek peninsula mountain barriers is the most important mechanism for deep convection, as discussed later in the text.
- The wind intensity exceeds 15 m s^{-1} within the warm south-easterly flow, along the eastern coasts of southern Greece (hatched areas in Fig. 11(b)).
- A progressive veering and weakening of the wind flow behind the cold-frontal zone (Fig. 11(b)). The cold-frontal surface is characterized by high relative vorticity (denoted by a shaded strip superimposed on the θ_e field (Fig. 11(a)) over the area south of Italy, where satellite imagery also revealed important cloud development (Fig. 3(a)).
- An advection of cold and dry air masses over the Balkans and northern Greece related to the high-pressure system over eastern Europe depicted in Fig. 2(a).

Figure 12(a) shows the condensation mixing ratio at the 850 and 400 hPa levels as well as the precipitation rate at the ground predicted by the RAMS on the outer grid at 0000 UTC 12 January. The cloud shield compares well with the infrared satellite picture (Fig. 3(a)) and the ECMWF vertical-velocity field (Fig. 3(b)), especially as it concerns the appearance of high convective clouds to the east of the main topographic axis of the Greek peninsula (dark shading in Fig. 12(a)) as well as the lack of vertical development along the west coasts of Greece and over the Aegean Sea. Some rain is also predicted from the northern part of the cold front in the area south of Italy. The heaviest precipitation rate in the RAMS outer grid is predicted over eastern continental Greece and the southern Aegean

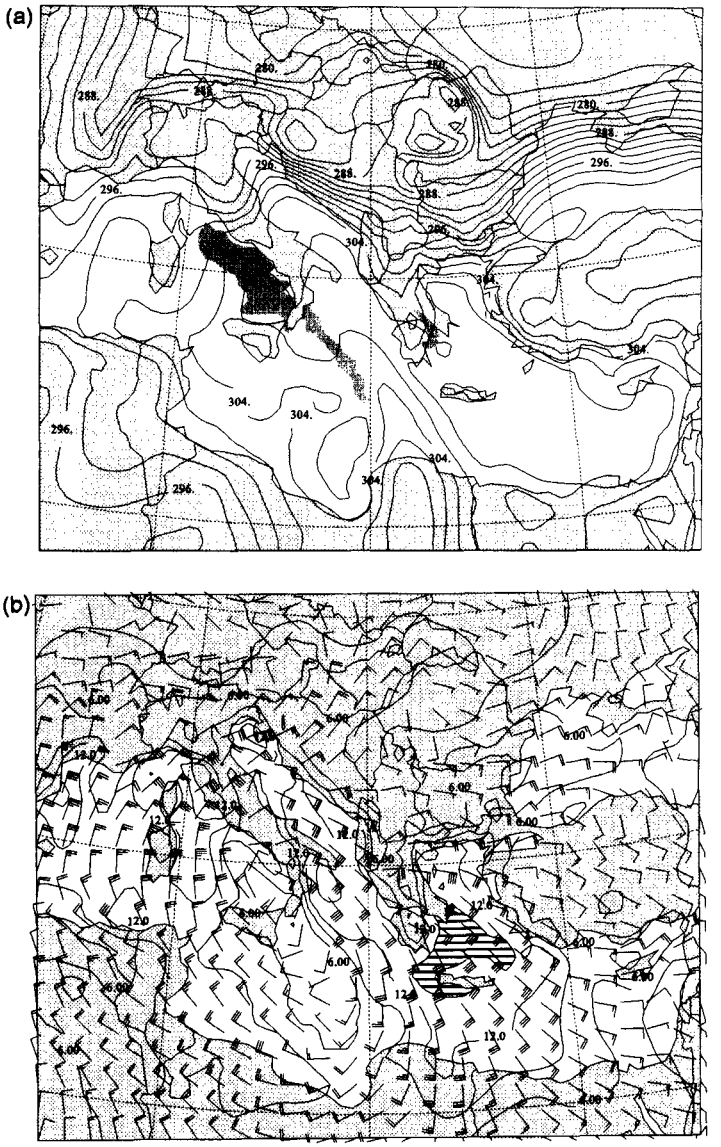

Figure 11. (a) The Regional Atmospheric Modeling System outer grid equivalent potential temperature (K) at the 925 hPa level, valid at 0000 UTC 12 January 1997. Dark shading denotes relative-vorticity values greater than 10^{-4} s^{-1}. (b) As (a) except for wind (at 3 m s^{-1} intervals, values greater than 15 m s^{-1} are hatched). Wind symbols are plotted every third grid point (one pennant: 20 m s^{-1}, one barb: 4 m s^{-1}, one half-barb: 2 m s^{-1}).

Sea, with a maximum over northern Peloponnisos, which is in good agreement with the observations.

A more realistic precipitation pattern is revealed on the second grid of the RAMS at the same time (Fig. 12(b)). Several clusters of heavy precipitation rate are evident over the eastern part of continental Greece, with the most prominent feature over the Korinthian Gulf, with a maximum of 23 mm h^{-1}. Indeed, at that time rain was reported at many stations located on the eastern coasts of continental Greece, with the heaviest rain reported over northern and eastern Peloponnisos (see hourly precipitation at Korinthos in northern

Peloponnisos, Fig. 9, with a peak of 33 mm h^{-1} at 0000 UTC 12 January). The model predicts well the area of high precipitation rate compared with the position of the highest cloud tops depicted on the infrared picture over this particular region (Fig. 3(a)). Note that the heaviest precipitation predicted by the RAMS is not over the mountain tops but at a distance upstream of the mountain slopes. This fact is consistent with previous investigations of mountain-related precipitation (Caracena *et al.* 1979; Yoshizaki and Ogura 1988). Indeed, in the presence of unstable air masses, when the LFC is lower than the mountain ridge precipitation occurs upstream but not at the mountain top. The role of topography on initiating deep convection and on the position and intensity of precipitation will be further discussed in the following sub-section. The precipitation band with light rain associated with the cold front itself is also evident in Fig. 12(b), from the area south of Italy and following a north-west/south-east axis. Precipitation reports are not available over the sea, but the model results do compare well with the satellite imagery of high cloud tops embedded in the rainband associated with the cold front (Fig. 3(a)).

At this stage it would be instructive to discuss the near-surface wind flow in the areas around the Korinthian Gulf, where the maximum precipitation rate occurred (Fig. 12(c)). The moist south-easterly near-surface flow of the order of 12 m s^{-1} is subject to frictional deceleration over the land of north-eastern Peloponnisos. Over the Korinthian Gulf the wind field is from variable directions, with a weak north-westerly flow over the eastern part of the Gulf, converging with the south-easterly flow at the area of maximum precipitation (over Korinthos). The only wind report over the Korinthian Gulf, during the night hours, was provided by a ship travelling eastwards along it. At 0000 UTC the ship was located at the western edge of the Gulf and reported an 8 m s^{-1} easterly wind (110°), but three hours later the same ship which at the time was over the central Korinthian Gulf reported a northerly wind (030°), and at 0600 UTC a 6 m s^{-1} wind from the 350° sector. The wind direction variability predicted by the model (and supported by the ship reports) over the Korinthian Gulf can be attributed to two factors:

(i) the complex terrain (indeed the Korinthian Gulf consists of a narrow strip of water, of 25 km width and about 100 km length, surrounded both from the north and south by high mountains, see Fig. 1(b)), which can produce descent over the Gulf; and

(ii) the low-level divergent flow associated with the descent behind the convective motions. Inspection of the low-level vertical-velocity field seems to support this hypothesis, as downward motions are predicted over the whole Korinthian Gulf, with the most important descent over its eastern part, just behind the position of the strong ascent (over the area of Korinthos). At levels higher than 500 m the wind field over the Gulf again presents a south-easterly direction over the whole domain, as shown in Fig. 12(c).

Twelve hours later the cold front reached southern Greece. The θ_e gradient on the 925 hPa level characterizing the cold front south of Peloponnisos over and south of Crete had strengthened during the elapsed 12 hours, exceeding 3 K in 100 km, while the 312 K isoline covered a large area from eastern Greece through the maritime area east of Crete and southwards over the south-eastern Mediterranean (Fig. 13(a)). The position of the frontal discontinuity over the Aegean Sea is delimited by a strip of high relative-vorticity values. The 925 hPa wind flow ahead of the front has also strengthened, exceeding 18 m s^{-1} over the southern Aegean (Fig. 13(b)), while at the lower model level (57 m above ground level) the wind exceeds 15 m s^{-1}, with a south-easterly direction (not shown). Strong easterly/north-easterly winds are also evident over the eastern coasts of northern continental Greece, exceeding 21 m s^{-1} (Fig. 13(b)).

As the cold front moved eastwards, reaching the Greek peninsula at 1200 UTC 12 January, an extended precipitation band oriented north-west/south-east developed over

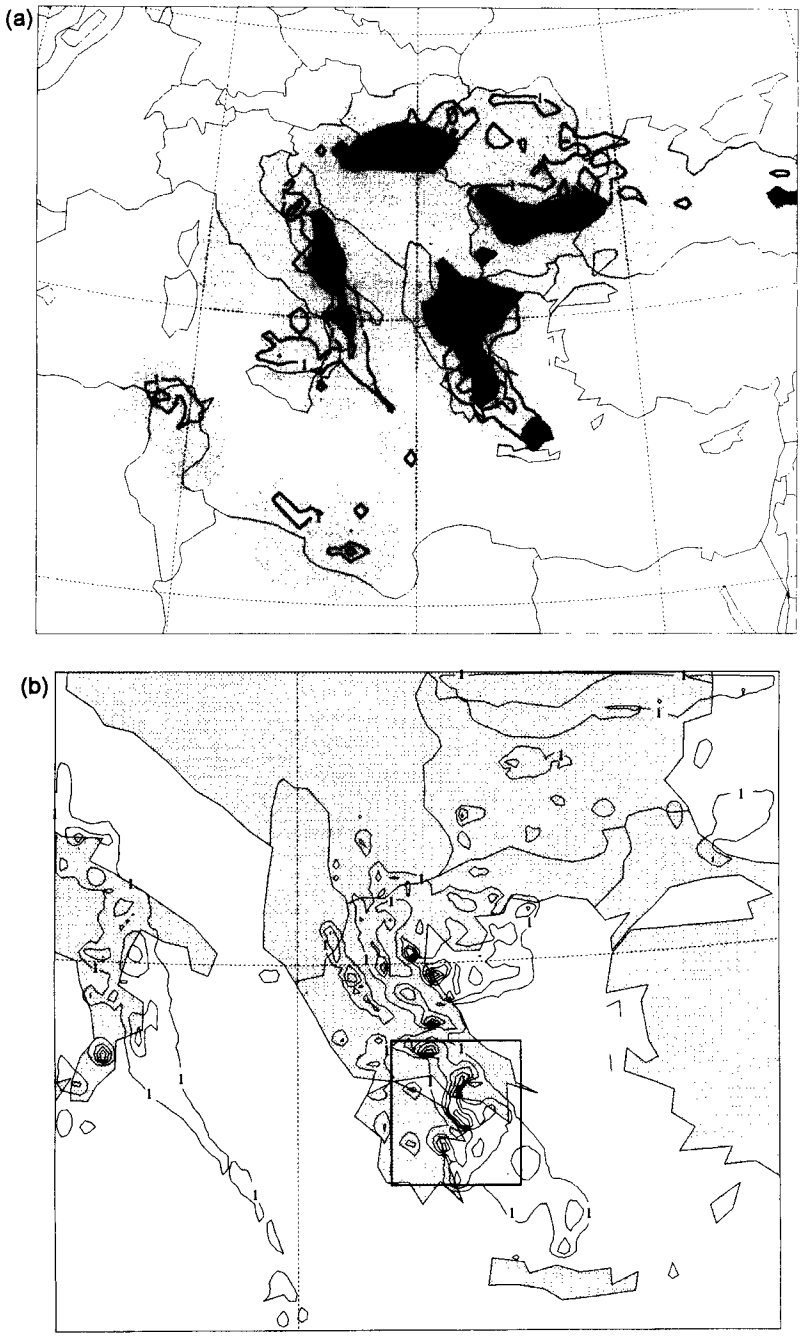

Figure 12. (a) The Regional Atmospheric Modeling System (RAMS) outer grid precipitation rate (at 4 mm h^{-1} intervals, first contour line is 1 mm h^{-1}) valid at 0000 UTC 12 January 1997. Superimposed are the 850 hPa condensation mixing ratio (light shading indicating values greater than 0.3 g kg^{-1}) and the 400 hPa condensation mixing ratio (dark shading indicating values greater than 0.3 g kg^{-1}). (b) The RAMS inner grid precipitation rate (at 4 mm h^{-1} intervals, first contour line is 1 mm h^{-1}) valid at 0000 UTC 12 January 1997. The rectangle represents the area reported in Fig. 12(c). (c) Wind field at $z = 57$ m above ground level in the area delimited by the rectangle in Fig. 12(b). Wind symbols are plotted every grid point (one pennant: 20 m s^{-1}, one barb: 4 m s^{-1}, one half-barb: 2 m s^{-1}). Topography is contoured every 300 m. The Korinthian Gulf is shaded. The city of Korinthos is denoted by KO.

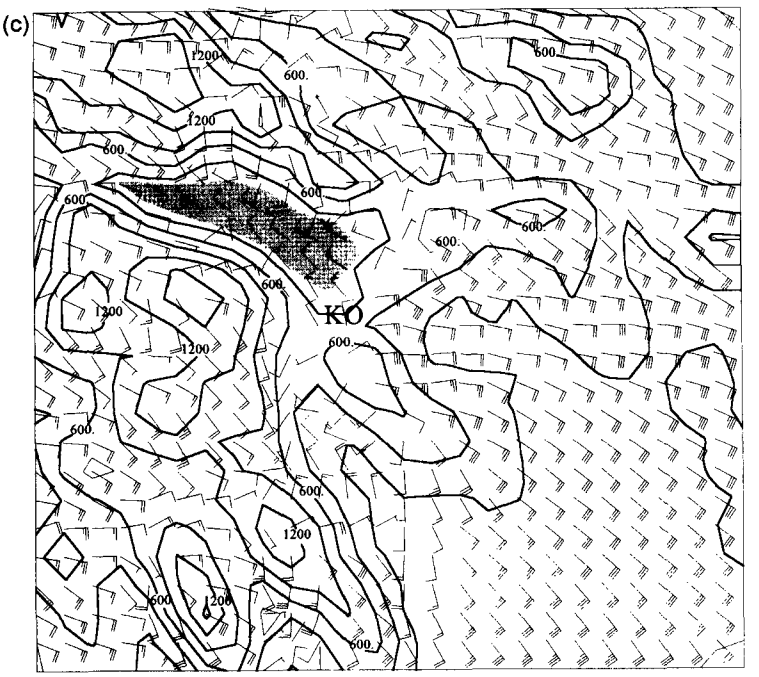

Figure 12. Continued.

eastern Greece and the Aegean Sea (not shown), in very good agreement with the cloud tops depicted in the satellite imagery (Fig. 7(a)). At this time ascent and deep convective clouds are reproduced by the model over an area following the position of the frontal discontinuity at the surface. Although the cold front did not produce heavy precipitation during its passage over the maritime area west of Greece, its actual position is optimal for deep convection, as the frontal activity is now accompanied by both increased moisture and further orographic lifting. At this time it is still raining over north-eastern Peloponnisos, but the most intense rainfall is now predicted over the southern part of central Greece where flooding was also reported. At this point it should be noted that inspection of the temporal variability of the reported precipitation rates from the rain-gauges implies that the model predicts a faster progression of the front (by about an hour) than actually happened.

At this point it is instructive to look through the 24-hour accumulated precipitation pattern ending at 1800 UTC 12 January, as this was predicted within the inner grid of the RAMS (Fig. 14), and compare it with the observed pattern presented in Fig. 1(c). It is clearly evident that rain was primarily accumulated along the eastern coasts of Greece and to a lesser extent over the Aegean Sea. The orographic enhancement and lee-side minima associated with the topography of the Greek peninsula appear to be simulated quite realistically. The heaviest precipitation amounts were predicted over the areas of flooding, especially over northern Peloponnisos and central Greece where the precipitation amount predicted by the RAMS exceeded 350 mm within 24 hours. This precipitation amount is in very good agreement with the measured amount of 305 mm at the Korinthos station. The predicted accumulated precipitation pattern compares quite well with the observed 24-hour accumulated precipitation, taking into account that the temporal and spatial variability of the precipitation field is very difficult to analyse objectively with a sparse rain-gauge network, especially in convective situations.

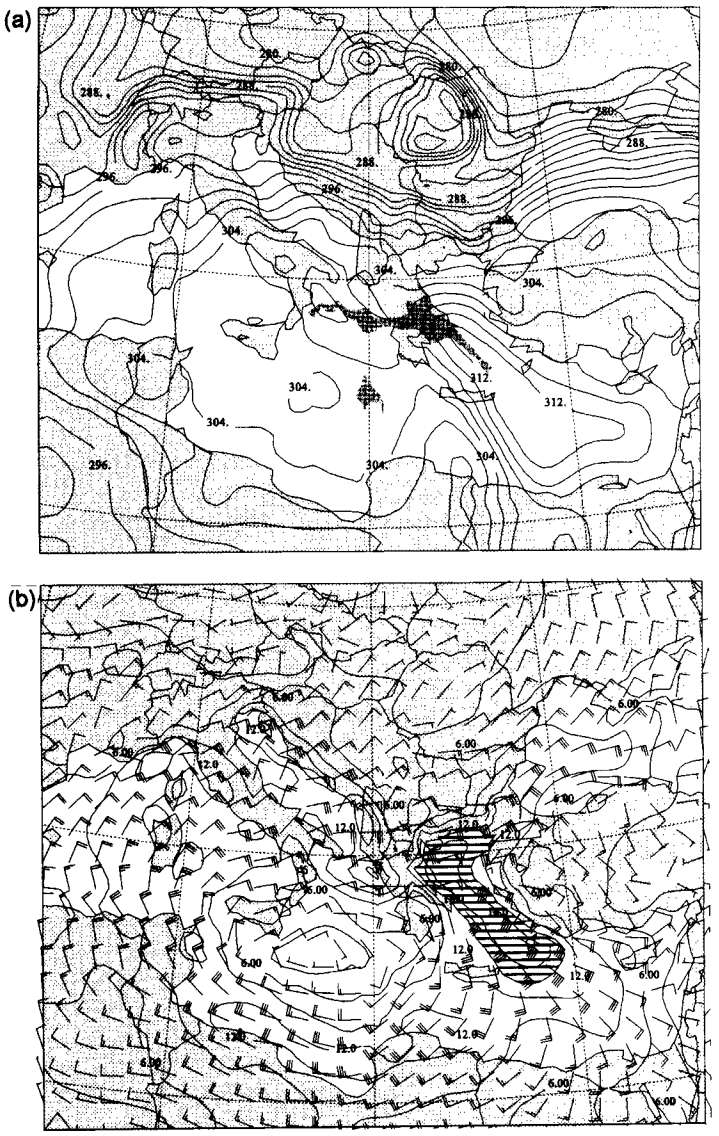

Figure 13. As Fig. 11 but for 1200 UTC 12 January 1997.

(c) *RAMS results—NOTOPO run*

Forced ascent of moist air up the slopes of a mountain barrier can lift the air directly to its LFC when the LFC at some inflow layer is near or below the level of the ridge top. Thunderstorms that grow in this way have produced spectacular results in the form of flash floods. Banta (1990) pointed out that in mountainous regions and when the LFC is below the height of the ridgeline, heavy rains occur midway up the windward slope. Maximum of precipitation midway up the windward slope has been reported by Caracena *et al.* (1979) and Yoshizaki and Ogura (1988) for the Big Thompson Flood over the USA, while Ogura *et al.* (1985) and Watanabe and Ogura (1987) reported orographically enhanced precipitation over the sea and the coast upwind of the mountains.

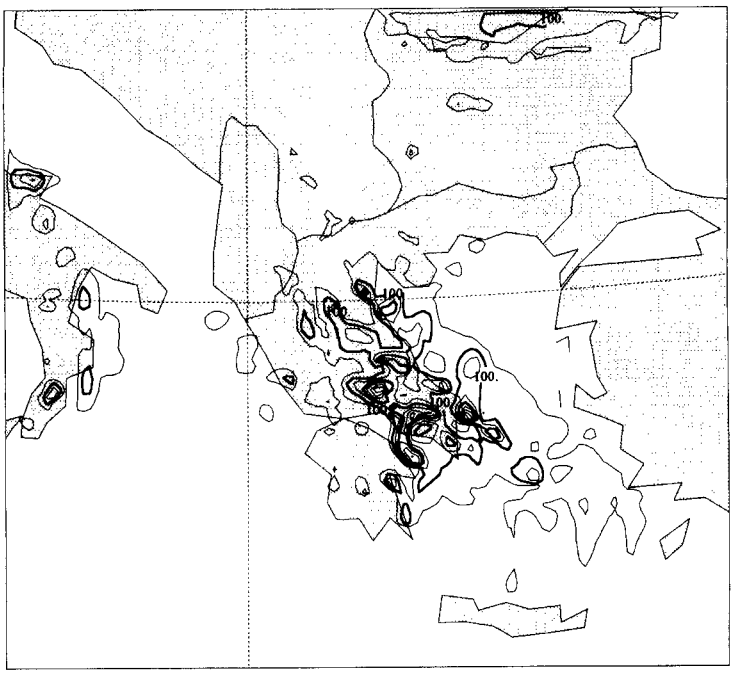

Figure 14. 24-hour accumulated precipitation ending at 1800 UTC 12 January 1997 (at 50 mm intervals), predicted inside the inner grid of the Regional Atmospheric Modeling System from the control simulation. The 100 and 200 mm contour lines are in bold.

During the flooding event analysed in this work the larger amounts of rain were accumulated at Korinthos and Desfina, located in upwind coastal regions rather than in a mountainous area. Despite the fact that no rain-gauge measurements are available over the mountainous areas, accumulated rain reported by the relatively sparse rain-gauge network in the upwind and downwind areas of the mountain ridges, along with satellite observations (Figs. 3(a) and 7(a)) and model results, support the idea that during this event the strong convective motions formed over the coastal areas upwind of the mountains, where it rained heavily, while it rained less on the higher mountains.

In order to examine the terrain-induced mechanisms involved in this severe-precipitation event, the same simulation (as described in section 3(a)) was performed where terrain was eliminated. As already mentioned, the effects of terrain on the initialization data as well as on the data used for nudging were eliminated as these fields were regenerated based on zero topography.

Before the arrival of the front over Greece, at 0000 UTC, the south-easterly flow within the warm conveyor belt penetrated inland over the Greek peninsula. Winds exceeding 15 m s^{-1} were predicted over the eastern part of the Greek peninsula and most of the Aegean Sea (not shown), compared with the blocking of this flow by the terrain in CONTROL. The condensate mixing ratio at 400 hPa revealed that there is some convective development over the western flank of the warm conveyor belt but it is restricted to central and northern Greece (not shown). This fact supports the idea that topography played a decisive role in the definition of the convective activity before the arrival of the front.

Later on, at 1200 UTC 12 January, the cold front reached the Greek peninsula. The wind flow just in front of the frontal discontinuity was strong with a south easterly direction over the Aegean Sea, and easterly over central Greece (not shown). The NOTOPO wind

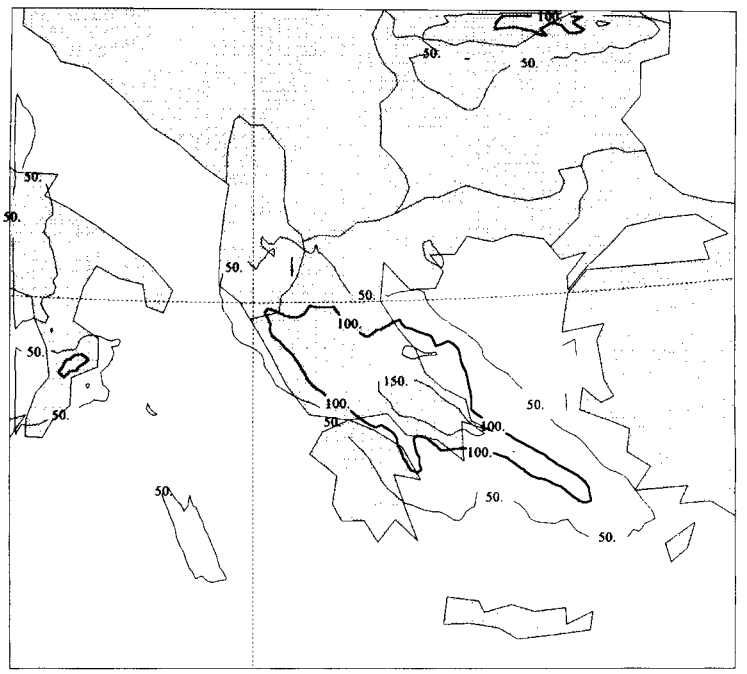

Figure 15. 24-hour accumulated precipitation ending at 1800 UTC 12 January 1997 (at 50 mm intervals), predicted inside the inner grid of the Regional Atmospheric Modeling System from the no topography simulation. The 100 mm contour line is in bold.

intensity is stronger than that of CONTROL and the resulting precipitation was substantially reduced. Indeed, inspection of the 24-hour accumulated precipitation at 1800 UTC (Fig. 15) reveals that the general precipitation pattern, following an axis oriented north-west/south-east, is reproduced by NOTOPO but with a maximum of 175 mm, compared with 305 mm for CONTROL (Fig. 14). Precipitation is smoothly distributed over the Greek peninsula and the Aegean Sea and it is associated with the cold-frontal lifting of the moist south-easterly low-level flow as well as to coastal convergence due to friction over land (note the relative rain enhancement over north-eastern Peloponissos compared with the rainfall of the maritime area just east of it). The NOTOPO accumulated precipitation for the period 1800–0000 UTC does not exceed 20 mm and it is homogeneously distributed over the eastern part of Greece, while CONTROL produced more than 80 mm within the same time period over the eastern part of the Korinthian Gulf (in good agreement with rain-gauge records shown in Fig. 9). Comparison of the accumulated precipitation produced by CONTROL and NOTOPO supports the idea that precipitation before the arrival of the front over the Greek peninsula is produced by the interaction of the south-easterly moist flow with the topography. Later on, when the front reached the area of interest, the observed precipitation was produced by the synoptic-scale lifting associated with the frontal passage, mainly over the sea, while further orographic lifting over land resulted in the enhancement of rainfall. Thus, orography played a decisive role in both the intensity and spatial distribution of rainfall.

4. Concluding remarks

In this study the Regional Atmospheric Modeling System (RAMS) is used along with all the available observations in order to study an extreme rainfall event which occurred

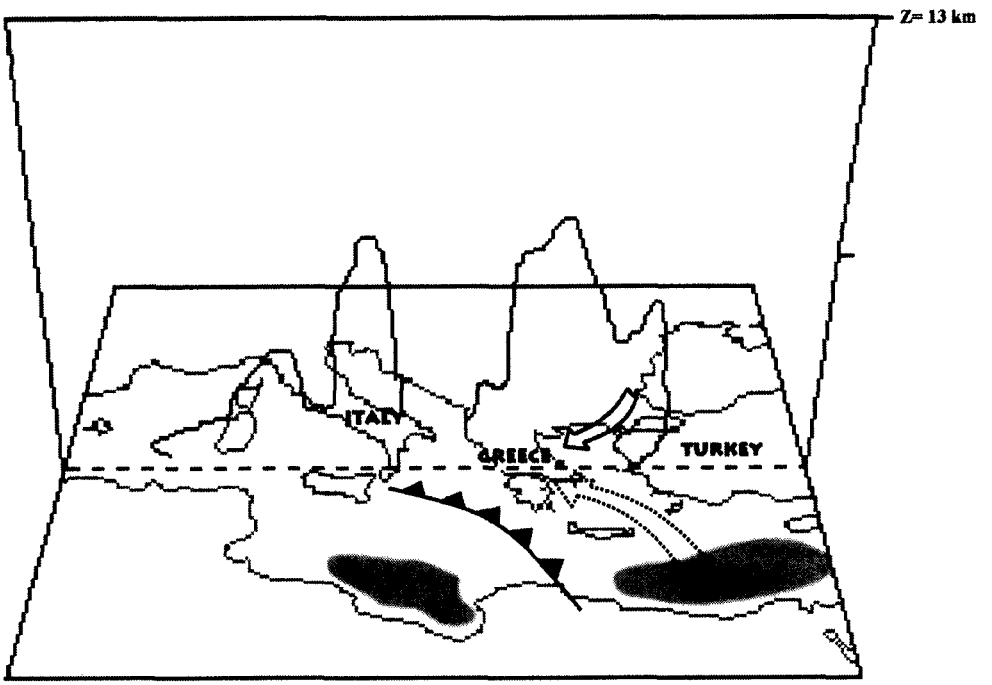

Figure 16. Vertical cross-section of the 0.3 g kg^{-1} condensation mixing ratio, valid at 0000 UTC 12 January 1997 (solid line). The low-level moist and dry wind flows are depicted with the dotted and the solid arrow, respectively. Shading denotes sea surface temperature exceeding 18 °C. The position of the cold front at the surface is denoted with conventional symbols.

on 11–12 January 1997. A characteristic feature of this event was that a large amount of precipitation (almost 50% of the 24-hour accumulated precipitation) was produced before the arrival of the front over the Greek peninsula. Observational and model analysis showed that the three factors considered as necessary for deep convection: instability, moisture supply and upward vertical velocity, were all met before the arrival of the front over the area of interest. Sounding reports showed that the atmosphere was ready to release its instability with only a little lifting, while the moisture supply was continuous by the south-easterly low-level flow with a long fetch over the warm Mediterranean waters. Topography then forced the near-surface moist flow to its LFC, producing severe convection. This feature was supported by the model results. Comparison between the zero topography (NOTOPO) simulation and the simulation control (where the real topography was used) revealed that the major amount of precipitation before the arrival of the front over the Greek peninsula was produced by orographic lifting.

The second interesting feature of the precipitation event was that the heaviest rainfall occurred over the coastal areas, upstream of important mountain barriers. This fact is consistent with previous investigations of mountain-related precipitation (Caracena *et al.* 1979; Yoshizaki and Ogura 1988) where in the presence of unstable air masses, when the LFC is lower than the mountain ridge, precipitation occurs upstream of, but not at, the mountain top. Indeed the soundings analysed during the event showed that the air masses were characterized by a low LFC and with a little lifting by the orography the air masses released their instability and produced heavy rain upstream from the mountains. This feature was evident in the sparse rain-gauge recordings but was further supported by the simulated precipitation pattern.

Model results allowed the construction of a conceptual scheme valid before the arrival of the cold front over Greece (Fig. 16) that represented the cloud development and low-level flow. It is obvious that the highest vertical extent of clouds is located over eastern continental Greece, where the moist south-easterly flow has been lifted by the orography.

A factor which played a role in the duration of the event was the high-pressure system prevailing over the Balkans which retarded the advance of the cold front, prohibiting its northward progression, and resulted in confining the moisture-rich south-easterly flow over southern and eastern Greece. The important convection over eastern Greece remained active during the whole night from 11 to 12 January, while the arrival of the front over the area produced a second maximum of rainfall over the already saturated soil and river catchments. The synergy of frontal convection and orographic lifting produced larger precipitation amounts in northern Peloponnisos and over central Greece. Devastating floods occurred in the city of Korinthos and over central Greece (in the Sperhios river catchment, near Lamia).

The analysis of such extreme-precipitation events can provide some understanding of the dynamics of these systems which can be useful to both researchers and forecasters. However, a better understanding of the small-scale structure of these storms for both research and nowcasting purposes can be gained through analysis of radar data. It is hoped that this will be achieved in the near future with the deployment of a network of weather radars in Greece.

Acknowledgements

The authors are grateful to the Hellenic National Meteorological Service and especially to Mr G. Potiriadis for providing the Meteosat data used in this study. Acknowledgement is also made to the National Center for Atmospheric Research, which is sponsored by the National Science Foundation (USA), for some of the computing time used in this research, and for providing the surface and upper-air data from the operational network used in this study (Contract number 35081178). Dr G. Sutherland (University of Athens) is acknowledged for his suggestions, which improved the English and grammar of the text.

References

Alpert, P., Neeman, B. U. and Shay-El, Y. 1990 Intermonthly variability of cyclone tracks in the Mediterranean. *J. Climate*, **3,** 1474–1478

Avissar, R. and Mahrer, Y. 1988 Mapping frost sensitive areas with a three-dimensional local scale numerical model. Part I: Physical and numerical aspects. *J. Appl. Meteorol.*, **27,** 400–413

Banta, R. 1990 The role of mountain flows in making clouds. *Meteorological Monograph*, **45,** 229–282

Barret, I., Jacq, V. and Rivrain, J.-C. 1994 A situation generating torrential rains in the Mediterranean area (the 22-23/09/93 stormy case in south-eastern France). (In French). *La Meteorologie*, **7,** 38–60

Brody, L. R. and Nestor, M. J. R. 1980 'Regional forecasts for the Mediterranean basin'. Technical report number 80-10. Naval Environmental Prediction Research Facility, Monterey, California, USA

Browning, K. A. and Pardoe, C. W. 1973 Structure of low-level jet-streams ahead of mid-latitude cold fronts. *Q. J. R. Meteorol. Soc.*, **99,** 619–638

Caracena, F., Maddox, R. A., Hoxit, L. R. and Chappell, C. F. 1979 Mesoanalysis of the Big Thomson storm. *Mon. Weather Rev.*, **107,** 1–17

Cotton, W. B., Thompson, T. and Mielke, P. W. 1994 Real time mesoscale prediction on workstations. *Bull. Am. Meteorol. Soc.*, **75,** 349–362

Davies, H. C. 1976 A lateral boundary formulation for multi-level prediction models. *Q. J. R. Meteorol. Soc.*, **102,** 405–418

Grossman, R. L. and Durran, D. R. 1984 Interaction of low-level flow with the western Ghat Mountains and offshore convection in the summer monsoon. *Mon. Weather Rev.*, **112,** 652–672

Lagouvardos, K., Kotroni, V., Dobricic, S., Nickovic, S. and Kallos, G. 1996 On the storm of 21–22 October 1994 over Greece: Observations and model results. *J. Geophys. Res.*, **101** (D21), 26217–26226

Lanzinger, A. 1997 'The January 1997 floods in Greece'. ECMWF Newsletter, **76,** 9–12

McCumber, M. C. and Pielke, R. A. 1981 Simulation of the effects of surface fluxes of heat and moisture in a mesoscale numerical model. Part I: Soil layer. *J. Geophys. Res.*, **86,** 9929–9938

Ogura, Y., Asai, T. and Dohi, K. 1985 A case study of a heavy precipitation event along the Baiu front in northern Kyushu, 23 July 1982: Nagasaki heavy rainfall. *J. Meteorol. Soc. Japan*, **63,** 883–900

Petroliagis, T., Buizza, R., Lanzinger, A. and Palmer, T. N. 1996 Extreme rainfall prediction using the European Centre for Medium-Range Weather Forecasts ensemble prediction system. *J. Geophys. Res.*, **101** (D21), 26227–26236

Pielke, R. A., Cotton, W. R., Walko, R. L., Tremback, C. J., Lyons, W. A., Grasso, L. D., Nicholls, M. E., Moran, M. D., Wesley, D. A., Lee, T. J. and Copeland, J. H. 1992 A comprehensive meteorological modelling system—RAMS. *Meteorol. Atmos. Phys.*, **49,** 69–91

Prezerakos, M., Flokas, H. and Michaelides, S. 1997 Absolute vorticity advection and potential vorticity of the free troposphere as synthetic tools for the diagnosis and forecasting of cyclogenesis. *Atmos.–Ocean*, **35,** 65–91

Senesi, S., Bougeault, P., Cheze, J.-L., Cosentino, P. and Thepenier, R.-M. 1996 The Vaison-La-Romaine flash flood: mesoscale analysis and predictability issues. *Weather and Forecasting*, **11,** 417–442

Tremback, C. J. 1990 'Numerical simulation of a mesoscale convective complex: Model development and numerical results'. Ph.D. dissertation, Colorado State University

Tremback, C. J., Lyons, W. A., Cotton, W. R., Walko, R. L. and Beitler, B. 1994 'Operational weather forecasting applications using the Regional Atmospheric Modeling System (RAMS)'. Preprints of the 10th conference on numerical weather prediction, Portland, OR, 18–22 July 1994

Walko, R. L., Cotton, W. R., Meyers, M. P. and Harrington, J. Y. 1995 New RAMS cloud microphysics parameterization. Part I: The single moment scheme. *Atmos. Res.*, **38,** 29–62

Watanabe, H. and Ogura, Y. 1987 Effects of orographically forced upstream lifting on mesoscale heavy precipitation: a case study. *J. Atmos. Sci.*, **44,** 661–675

Yoshizaki, M. and Ogura, Y. 1988 Two- and three-dimensional modeling studies of the Big Thompson storm. *J. Atmos. Sci.*, **45,** 3700–3722